Central European Journal of Energetic Materials, **2015**, *12*(1), 159-174
ISSN 2353-1843

Modelling of the Viscoplastic Behaviour of Homogeneous Solid Propellants

Mariusz PYRZ [1], Robert ZALEWSKI [2]

[1] *Warsaw University of Technology, Institute of Vehicles, Warsaw, Narbutta 84, Poland*
[2] *Warsaw University of Technology, Institute of Machine Design Fundamentals, Warsaw, Narbutta 84, Poland*
E-mails: mpyrz@simr.pw.edu.pl; robertzalewski@wp.pl

Abstract: This study is concerned with the mechanical properties of homogenous solid propellants. The experimental results demonstrate the high strain rate sensitivity of these materials. A modified viscoplastic model of the Bodner-Partom type was applied to simulate the nonlinear behaviour of solid propellants when subjected to uni-axial loading conditions. The material parameters of the constitutive law were identified numerically using the evolutionary algorithm. The capability of the proposed approach was investigated for a representative solid fuel sample. The efficiency of the method is discussed.

Keywords: solid propellants, experiments, modelling, parameter identification, evolutionary algorithms

1 Introduction

Investigations of homogeneous solid propellants, which belong to the group of thermoplastic materials, can provide very important information related to their mechanical properties. The mechanical characteristics of homogeneous energetic materials enable the operational properties of these materials to be effectively predicted and evaluated. Such information is especially important when a solid propellant is subjected to cyclic dynamic loading resulting from transportation, operation and particularly non-stationary burning processes.

The mechanical response of homogeneous solid rocket propellants under

different types of loading depends on the physical and chemical changes observed in these materials. In the case of double-base homogeneous solid propellants, dynamic mechanical analysis (DMA) is very helpful. It can provide important parameters such as dynamic loss modulus, dynamic storage modulus, tangent of the angle of phase shift between the mentioned moduli (damping coefficient) and the relative dynamic strain for these materials. The problem becomes much more complicated for propellants having a complex structure. In these cases classical strength experiments, carried out on specially formed test specimens of the solid propellants, are generally performed.

Former works [1, 2] have shown that homogenous solid propellants exhibit "non-classical" mechanical behaviour, *i.e*. nonlinear and, in some ways, similar to certain polymers. Analogous properties have also been observed in [3, 4]. Furthermore, the behaviour is strongly affected by such factors as temperature [5, 6], strain rate [7, 8] and high energy fuel additives [9]. Numerical modelling of such phenomena can complement the experimental studies and contribute to the understanding and prediction of the complex behaviour of these nonclassical materials.

In the last two decades, a great deal of effort has been applied to the viscoplastic modelling of thermoplastic materials [10, 11]. Generally, the viscoplastic models can be divided into phenomenologically and physically based models (however even in the latter class of models, some parameters do not have a direct physical meaning). Deformation processes in polymer-like materials, exemplified by homogeneous solid propellants, are not understood very well, even in a qualitative manner. The problem is very often described phenomenologically with regard to the basic principles of thermodynamics of continuous media, and by introducing adequate internal variables.

Different models developed for metals can also be used for the description of the nonlinear behaviour after yielding of thermoplastic materials [12-14]. However, the investigation of the viscoplastic response of such materials is still challenging. Furthermore, the problem of how to evaluate the proper values of the material parameters is unsolved. In fact, all nonlinear viscoplastic models involve a large number of parameters, which often leads to ambiguous identification results. The experimental determination of material constants can be very complicated for the entire range of possible applications (*e.g*. in terms of strain rates or temperatures), and usually demands sophisticated and expensive experimental conditions. At the same time, great accuracy of these values is necessary in order to extrapolate the numerical results in a realistic manner beyond the experimental range. In practice, only a limited number of experimental tests can be conducted, carried out for a restricted range of strain rates and temperatures.

In the present work, the modelling and the identification of viscoplastic parameters of constitutive equations for selected examples of homogeneous solid propellants is considered. From the large number of viscoplastic laws presented in the literature, the modified Bodner-Partom (B-P) model has been chosen. The original version of the B-P viscoplastic model [15] does not allow us to describe the softening phenomenon after the ultimate strength point, observed for various types of homogeneous solid propellants. The modified formulation of the B-P model investigated in the paper was proposed in [12] for the simulation of polymer behaviour under different strain rates.

In this paper, a typical homogeneous solid propellant testing specimen was investigated experimentally at various strain rates and at a constant temperature. The capability and usefulness of the proposed viscoplastic model was analyzed. The stochastic search method based on evolutionary algorithms was developed to evaluate the values of the material parameters. A number of different experimental curves was taken into account in the proposed numerical identification strategy. The efficiency of the modelling is discussed and perspectives for further research are presented.

2 Experiments

The aim of the laboratory tests was to determine the mechanical properties of the chosen energetic materials. In the first stage, the response of homogeneous solid rocket propellants to various strain rates was investigated. The experimental results were intended to provide suitable data for the selection of an appropriate constitutive model.

The experiments began with uni-axial tensile tests carried out at constant temperature T = 293 ± 2 K and humidity (65 ± 5%) conditions.

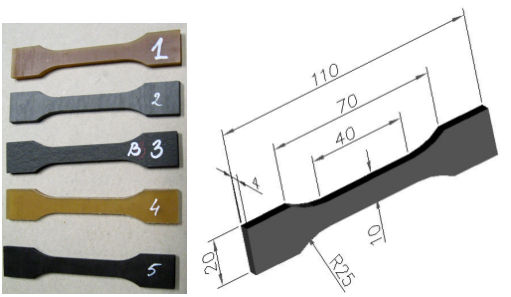

Figure 1. Homogeneous solid propellant experimental samples (dimensions in mm).

A universal tensile strength machine INSTRON 4500 was used. The device was equipped additionally with a thermal chamber that enabled tests at various temperatures to be conducted. The experimental program included the investigation of five different homogeneous solid rocket propellant materials (trade names: Agate, Basalt, Marble, Sapphire and Emerald). Laboratory tests were performed on dumbbell shaped specimens (Figure 1) and at four different strain rates (0.000185, 0.00185, 0.0185 and 0.075 s^{-1}). At least three independent experimental series for each material were conducted to eliminate the influence of gross error. The average values of correctly performed experiments were taken as the final result.

Typical results of the uni-axial tension tests are presented in Figures 2 and 3.

A comparison of the laboratory results depicted in Figures 2 and 3 reveals substantial qualitative and quantitative differences between the experimental curves obtained for the same type of homogeneous solid propellant.

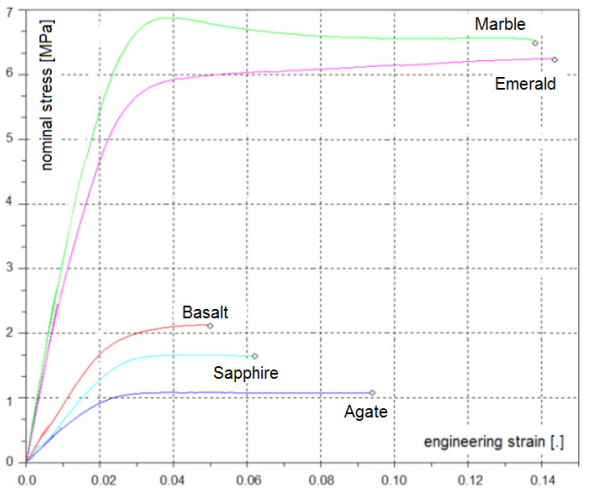

Figure 2. Stress-strain curves for different solid propellants (constant strain rate 0.000185 s^{-1} and temperature T=294 K).

A more precise analysis reveals that the impact of the experimental strain rate on the mechanical properties of the materials considered is also different. Although the effect of the strain rate is evident for all propellants, the sensitivity of a material's response to loading velocity changes is different. Furthermore the elongation and elasticity modulus values are different. This effect, resulting from the chemical composition and the fabrication process, makes analysis of the mechanical properties of homogeneous solid propellants much more complex than classical materials.

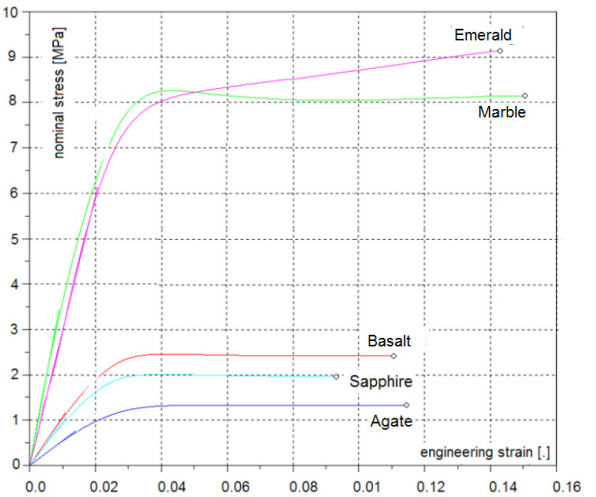

Figure 3. Stress-strain curves for different solid propellants (constant strain rate 0.00185 s^{-1} and temperature T=294 K).

It should be emphasized that the shape of the experimental stress-strain curve for the Marble specimen differs from the others. In both Figures 2 and 3, we can observe that the behaviour of that propellant reveals a softening phenomenon consisting of a decreasing stress-strain curve for higher values of plastic deformation. This feature had a strong influence on the selection of the constitutive model. It was shown in [2] that such a softening effect is observable for selected homogeneous solid propellants and depends strongly on the temperature.

3 Constitutive Model

Quantitative modelling of the general plastic response of nonclassical materials is a rather delicate question. Since the behaviour of the material under consideration is similar to the hardening curves of a glassy polymer, the authors of the present paper decided to adopt some analogous phenomenological constitutive equations proposed in the literature. One of the commonly used models is the B-P law [15], based on the assumption of strain rate **D** additivity and its decomposition into an elastic $\mathbf{D}^e$ and an inelastic $\mathbf{D}^p$ part:

$$\mathbf{D} = \mathbf{D}^e + \mathbf{D}^p \tag{1}$$

The elastic strain rate tensor $\mathbf{D}^e$ is given by the time derivative of the generalized Hooke's law:

$$\dot{\boldsymbol{\sigma}} = \mathbf{C} : \mathbf{D}^e \tag{2}$$

where $\dot{\boldsymbol{\sigma}}$ is the time derivative of the Cauchy stress tensor and $\mathbf{C}$ is the fourth-order isotropic elastic modulus tensor.

The inelastic strain rate tensor $\mathbf{D}^p$ is given by the following explicit function:

$$\mathbf{D}^p = \frac{2}{3}\dot{p}\frac{\boldsymbol{\sigma}'}{\sigma_{eq}} \tag{3}$$

where $\dot{p}$ is the accumulated inelastic strain rate, σ_{eq} is the equivalent stress and $\boldsymbol{\sigma}'$ is the deviatoric stress defined respectively as:

$$\dot{p} = \left(\frac{2}{3}\mathbf{D}^p : \mathbf{D}^p\right)^{1/2},\ \sigma_{eq} = \left(\frac{3}{2}\boldsymbol{\sigma}' : \boldsymbol{\sigma}'\right)^{1/2},\ \boldsymbol{\sigma}' = \boldsymbol{\sigma} - \frac{1}{3}tr(\boldsymbol{\sigma})\mathbf{I} \tag{4}$$

The accumulated inelastic strain rate of the original B-P model [15] has been defined by the following exponential function:

$$\dot{p} = \frac{2}{\sqrt{3}} D_0 \exp\left(-\frac{1}{2}\left(\frac{Z_1 + Z_2}{\sigma_{eq}}\right)^{2n}\right) \tag{5}$$

where D_0 is the limiting shear strain rate, and n is the strain rate sensitivity parameter. The internal state variables Z_1 and Z_2 characterize the isotropic and the kinematic hardening respectively. The complete definition of the B-P model requires the estimation of the values of numerous material parameters, which can be as many as 14. If the unified B-P model has no yield surface, then the inelastic strain rate exists from the beginning of loading.

In this paper we will apply the modified version of the B-P law [12, 13], denoted as MBP in the following. The model has been adapted to the particular mechanical response of materials characterized by a peak at the yield stress, followed by intrinsic strain hardening. In this version the specific form of the accumulated inelastic strain rate of the MBP model is written as:

$$\dot{p} = \frac{2}{\sqrt{3}} D_0 \left(\frac{\sigma_{eq}}{Z_3 + Z_4} \right)^{2n} \tag{6}$$

where D_0 and n are the same terms as defined earlier, Z_3 is an internal variable introduced to take into account the effect of strain softening:

$$\dot{Z}_3 = m_3 (Z_{3s} - Z_3) \dot{W}^p \tag{7}$$

and Z_4 is an internal variable introduced to take into account the effect of strain hardening:

$$\dot{Z}_4 = m_4 \left(\frac{Z_4 - (1-\alpha) Z_{40}}{Z_{40}} \right) \dot{W}^p \tag{8}$$

In Equations (7) and (8) Z_{40}, directly related to the yield stress, is the initial value of Z_4, Z_{3s} is the saturation value of Z_3, α is a hardening parameter controlling the beginning of the strain hardening, and m_3 and m_4 are the softening and hardening rate parameters, respectively.

The initial conditions on the internal variables Z_3 and Z_4 are:

$$Z_3(0) = 0,\ Z_4(0) = Z_{40} \tag{9}$$

According to [16] the parameter D_0 is arbitrarily selected as $D_0 = 10^4\ s^{-1}$ in static mode. Finally, the proposed MBP model of material behaviour (investigated at room temperature) involves six internal material parameters: n, Z_{40}, m_3, m_4, Z_{3s}, α. Their values have to be identified on the basis of experimental data. The analytical methodologies for identification demand advanced expertise in the formulation of constitutive laws and significant experience in the understanding of experimental material. In this work the parameter values were determined using numerical methods.

4 Numerical Estimation of Material Parameters

In this section we formulate the identification procedure as an optimization problem. The values of the material parameters for the MBP model can be evaluated by comparison of experimental and numerical curves, so as to

obtain the minimal discrepancy between them. The objective function can be formulated as the sum of the errors between the experimental and the simulated characteristics, calculated at selected points in the investigated domain. Hence, the curve fitting problem, related to the model calibration, is represented as a minimization problem.

In the general formulation of the parameter identification, we have to determine N material constants $c_1,\ldots,c_N$ of the constitutive model so as to minimize the sum S of the differences between the measured experimental data p^{exp} and the computed results p^{num} at M given points in the experimental domain:

$$S\left(c_1,...,c_N\right)=\sum_{i=1}^{M}\left|p_i^{exp}-p_i^{num}\left(c_1,...,c_N\right)\right|\rightarrow \min. \tag{10}$$

In the problem under consideration, the difference between the experimental and the numerical curves is expressed in terms of the stress values (σ_i^{exp}, σ_i^{num} respectively), corresponding to strains ε_i^{exp} at experimental points i ($i = 1, ..., M$). Moreover, the average discrepancy per point is taken in order to normalize the value of S. The corresponding objective function takes the form:

$$S\left(c_1,...,c_N\right)=\frac{1}{M}\left(\sum_{i=1}^{M}\left|\sigma_i^{exp}-\sigma_i^{num}\left(c_1,...,c_N\right)\right|\right)\rightarrow \min. \tag{11}$$

In the case of several experimental curves being simultaneously taken into consideration in the identification procedure, the objective function value S is calculated at all of the comparison points of all of the curves.

The solution of the optimization problem (11) is not generally a trivial task. Several classical minimization algorithms, based essentially on gradient estimation, may be applied, but the corresponding inverse problem is not so easy to solve because of the mathematical complexity of the formulation and the number of parameters and the unknown range of their variation. An interesting alternative is the use of nondeterministic search methods, as for example Evolutionary Algorithms (EA), inspired by natural evolution, hereditary and survival of the fittest [17]. The method is naturally adapted to unconstrained optimization and is efficient in difficult, large size, high cardinality and multimodal problems. EAs have been applied with success to a large variety of optimization problems and have become a recognized solving methodology, in spite of its random character and the relatively large number of objective function evaluations which are necessary to guarantee convergence.

The EA developed for this study, uses the floating point, natural representation of the design variables. In consequence, no encoding and decoding techniques

are necessary for the searched values. An N-parameter constitutive law problem is represented directly by a string of N material constants c_i (i = 1, ..., N). Each optimization variable is allowed to vary within limits fixed by the user. The quality of a potential solution is represented by the fitness f. In this study the following definition has been applied:

$$f = \frac{C}{S(c_1,...,c_N)+1} \tag{12}$$

where the average difference per experimental point between the experimental stress and the numerical simulation stress values S is given by Equation (11), C is a scaling coefficient and the unity term in the denominator is included to prevent the singularity of the expression.

EAs have already been applied to the identification problems of viscoplastic behaviour of different classical and non-classical materials. For example in [18], the Genetic Algorithm-based multiple objective optimization procedure was applied to determine the unified viscoplastic constitutive equations for superplastic alloys. In previous papers, the authors studied the mechanical response of polymers and vacuum packed particles, and used EAs for the parametric identification of constitutive models [19, 20]. In the present study we followed this direction, and investigated the particular behaviour of homogenous solid propellant materials.

5 Numerical Examples

The numerical examples demonstrate the ability of the MBP constitutive model to emulate the behaviour of a typical solid propellant material (Emerald). To determine the yield behaviour of the selected solid propellant, experimental samples were investigated at four different strain rates (0.000185, 0.00185, 0.0185 and 0.075 s^{-1}) at room temperature. The Young's modulus value E = 360 MPa was numerically determined based on the initial, linear part of the stress-strain curve.

In the EA identification procedure, the behaviour of the material was simulated in the strain range from 0 to 0.014. Fifteen reference comparison points, uniformly located in the domain investigated, were taken into account for each experimental data set.

5.1 Calibration using a single reference curve

The six material parameters n, m_4, α, Z_{40}, Z_{3s}, m_3 of the modified MBP model were

searched numerically using the optimization criteria (11) and the fitness function (12). In preliminary tests the parameter variations were investigated at relatively large variation intervals. Subsequently, the extreme zones of the research space were cut off and the parameters searched within the following limits: $1 \leq n \leq 20$, $10 \leq m_4 \leq 150$, $0.001 \leq \alpha \leq 0.5$, $30\ \text{MPa} \leq Z_{40} \leq 180\ \text{MPa}$, $-30\ \text{MPa} \leq Z_{3s} \leq -1\ \text{MPa}$, $1\ \text{MPa}^{-1} \leq m_3 \leq 20\ \text{MPa}^{-1}$. The EA was applied to a population of 100 individuals, used the "single" arithmetical crossover operator (applied with probability 0.7), and the non-uniform mutation (with probability 0.15). One hundred generations were investigated and the selection procedure employed tournament ranking using randomly assigned pairs. Moreover, the elitist strategy replaced the two worst individuals in the new generation by the two best individuals found in the previous generation. In order to complete the study of the efficiency of the EA identification, the program was run independently 20 times and the average values were analyzed.

The first examples were performed by taking only one experimental curve in the identification procedure. We began with the reference curve corresponding to the lowest strain rate experiment $\dot{\varepsilon} = 0.000185\ \text{s}^{-1}$. The best result (in terms of the fitness) corresponded to the values: $n = 2.69$, $m_4 = 92.71$, $\alpha = 0.171$, $Z_{40} = 165.71$ MPa, $Z_{3s} = -13.58$ MPa, $m_3 = 2.062\ \text{MPa}^{-1}$. This is presented in Figure 4, where, additionally, the behaviour for all of the experimental strain rates has been simulated. In order to facilitate the interpretation, only the experimental "comparison" points have been plotted with markers, the numerical simulation results being presented as continuous lines. One can see that the applied MBP law accurately follows only the experimental results used for the model calibration. The material behaviour was not well approximated for the experiments performed at the higher strain rate $0.00185\ \text{s}^{-1}$, and diverges for other strain rates. The reason for this is that the identification procedure minimized only the difference between the numerical curve generated for $\dot{\varepsilon} = 0.000185\ \text{s}^{-1}$ and the corresponding set of experimental points. The average difference per "comparison" point (of one reference curve) was relatively small and equal to 0.11 MPa. However the average discrepancy (per comparison point), calculated for four modelled curves, greatly exceeded 2 MPa. In the case of the two highest strain rate curves one notices the smooth softening effect which it is possible to obtain using the MBP model.

Similar behaviour was observed for other identification examples, carried out (separately) for experimental results corresponding to strain rates of 0.00185, 0.0185 and $0.075\ \text{s}^{-1}$. The results of the modelling are presented in Figures 5, 6 and 7, respectively. For example, the solution obtained on the basis of experiments corresponding to the "highest" reference curve $\dot{\varepsilon} = 0.075\ \text{s}^{-1}$ is

presented in Figure 7 (with $n = 2.68$, $m_4 = 38.09$, $\alpha = 0.202$, $Z_{40} = 125.89$ MPa, $Z_{3s} = -12.22$ MPa, $m_3 = 14.53$ MPa^{-1}). In that case only the reference experimental points are well approximated. The identification procedure enabled us to fit quite well the stress-strain relation chosen for the identification procedure, though the approximation of the remaining experimental tests is not very precise and may diverge significantly for the other strain rate curves. This is due to the fact that the single reference curve considered in the numerical identification procedure is not sufficient to capture the viscosity effect existing in the homogeneous solid propellants investigated. Moreover, similar values of the objective function (12) can be obtained for relatively different sets of internal state variables.

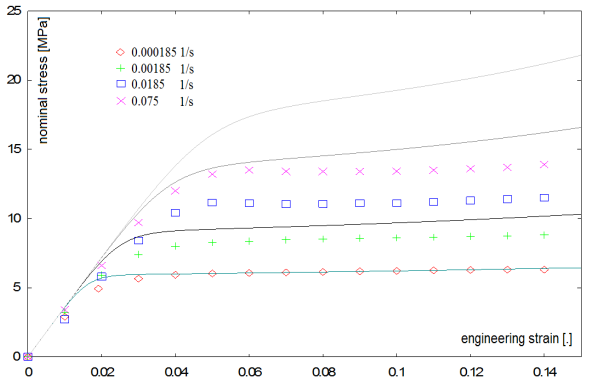

Figure 4. Results of the MBP model calibrated using a single experimental test $\dot{\varepsilon} = 0.000185$ s^{-1}.

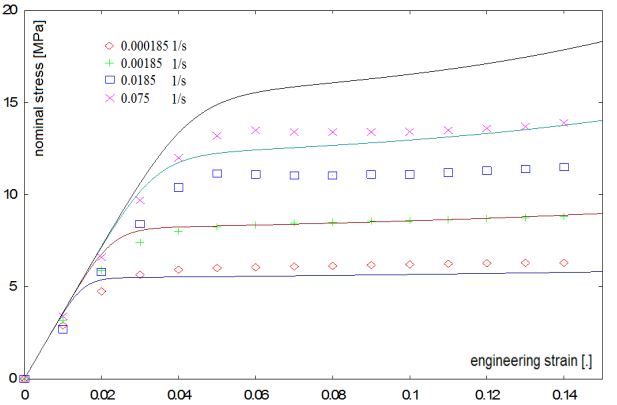

Figure 5. Results of the MBP model calibrated using a single experimental test $\dot{\varepsilon} = 0.00185$ s^{-1}.

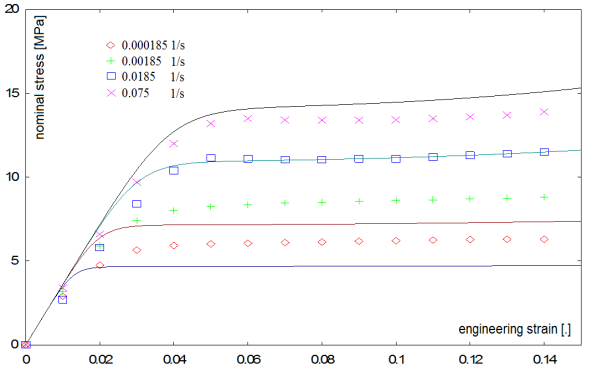

Figure 6. Results of the MBP model calibrated using a single experimental test $\dot{\varepsilon} = 0.0185$ s^{-1}.

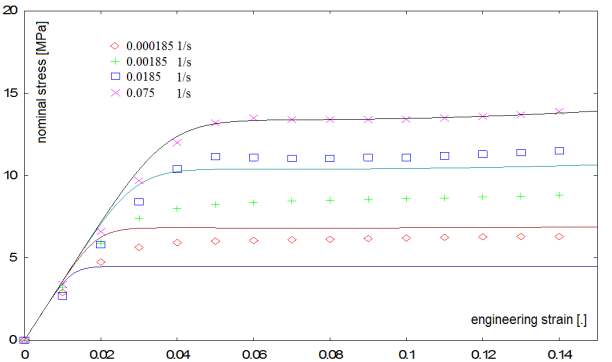

Figure 7. Results of the MBP model calibrated using a single experimental test $\dot{\varepsilon} = 0.075$ s^{-1}.

5.2 Calibration using two reference curves

The next identification example was carried out by simultaneously minimizing the disparities with respect to two experimental curves in the definition of the objective function (12). The extreme strain rate curves were chosen corresponding to experimental data obtained for $\dot{\varepsilon} = 0.000185$ s^{-1} and $\dot{\varepsilon} = 0.075$ s^{-1}. This time the results of the simulation were much better than those obtained in the previous section. An example of the simulation is depicted in Figure 8. It corresponds to $n = 3.61$, $m_4 = 82.77$, $\alpha = 0.046$, $Z_{40} = 72.30$ MPa, $Z_{3s} = -22.06$ MPa, $m_3 = 10.35$ MPa^{-1}. The numerical curves obtained remain close to the experimental points. The average difference per "comparison" point (for two curves taken together) was equal to 0.275 MPa. If one takes into account all four modelled

curves, the error becomes larger and exceeds 0.370 MPa per comparison point. The use of two different experimental results enables us to capture the strain rate sensitivity and to better calibrate the model in the identification procedure.

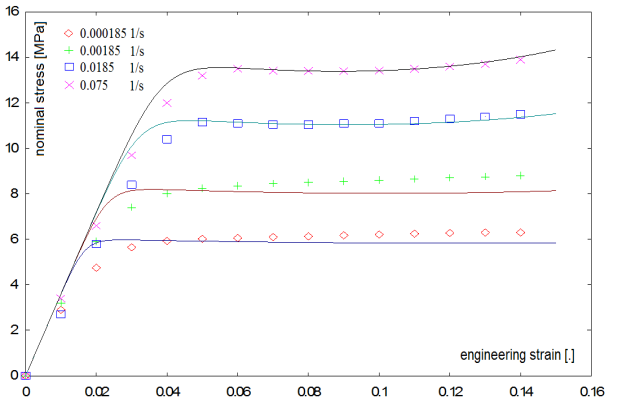

Figure 8. Results of the MBP model calibrated using two experimental curves $\dot{\varepsilon} = 0.000185\ s^{-1}$ and $\dot{\varepsilon} = 0.075\ s^{-1}$.

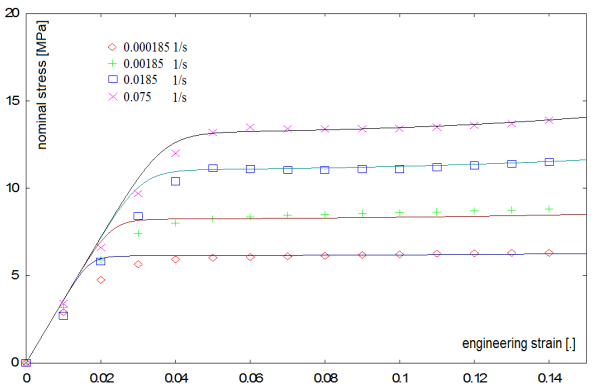

Figure 9. Results of the MBP model calibrated using four experimental curves.

5.3 Calibration using four reference curves

In this example four experimental data curves were included in the objective function and the MBP model was calibrated by searching the minimal value of the discrepancies at all "comparison" experimental points of all curves. In order to verify the effectiveness of the AE approach, as well as the consistency of the results, the identification procedure has been run independently 20 times. The average values of the parameters were calculated and inserted into the

constitutive relation. The result of the simulation is presented in Figure 9 and corresponds to the following set of internal state variables: $n = 3.89$, $m_4 = 46.92$, $\alpha = 0.052$, $Z_{40} = 61.27$ MPa, $Z_{3s} = -12.02$ MPa, $m_3 = 1.846$ MPa^{-1}. In this case the average difference per "comparison" point (for all four curves taken together) was equal to 0.235 MPa. Due to the four different sets of experimental results, the strain rate sensitivity of the homogeneous solid propellants investigated has been captured exactly and resulted in the precise calibration of the MBP model.

6 Conclusions

The investigation of the properties of solid propellants has been ongoing for several years. In devices operating with solid propellants, the burning event is quite complex. The physico-mechanical processes occurring during burning are not fully recognized.

In this work, the elastic-viscoplastic behaviour of a typical solid propellant was studied. The modified Bodner-Partom (MBP) constitutive law has been applied to model the inelastic deformation of the investigated material in uni-axial tensile tests. Comparisons between the model and the experimental results have shown the capacity of the model to take into account the highly nonlinear behaviour and rate-dependence of the studied material. The material parameters were determined numerically. The identification problem was formulated as an optimization task and solved using an Evolutionary Algorithm (EA) developed for this study.

The EA approach is a stochastic search method, but its efficiency in the inverse problem of the identification of material parameters for the propellants considered is very satisfying. The main drawback of this methodology resides in a large number of potential solutions that have to be investigated in order to obtain the final result. In the examples presented, the CPU time was really small, and varied between 30 and 90 seconds (for the most time-consuming example of four experimental curves taken simultaneously) on a personal computer. This search method proposes a set of parameters, which can vary a little due to the stochastic nature of the EA strategy, but always correctly fit the experimental results. The approach presented can be easily adapted to other constitutive laws and used to investigate "new" materials.

Based on the experimental and numerical analyses presented in this paper, it can be stated that for the precise calibration of the MBP model, at least two uni-axial tensile tests at various strain rates should be carried out. In order to obtain the best convergence between the real and simulated responses of the

material, possibly extreme values of the strain rates should be taken into account in the laboratory tests.

In further studies, the methodology presented here will be applied to the analysis of different constitutive models and to the investigation of other aspects of solid propellants, such as temperature, former loading history, cyclic loading or environmental impact. The precise description of this complex behaviour may require more advanced models [21-23] and additional experiments in order to carry out the calibration process correctly and to ensure the uniqueness of the resulting solution.

7 References

[1] Zalewski R., Wolszakiewicz T., Analysis of Uniaxial Tensile Tests for Homogeneous Solid Propellants under Various Loading Conditions, *Cent. Eur. J. Energ. Mater.*, **2011**, *8*(4), 223-231.

[2] Zalewski R., Wolszakiewicz T., Experimental Research of Fundamental Mechanical Properties of Homogeneous Solid Rocket Propellants, *Przemysl Chemiczny*, **2012**, *91*(9), 1825-1829.

[3] Ho S.-Y., High Strain-Rate Constitutive Models for Solid Rocket Propellants, *J. Prop. Power*, **2002**, *18*(5), 1106-1111.

[4] Shekhar H., Kankane D. K., Viscoelastic Characterization of Different Solid Rocket Propellants Using the Maxwell Spring-Dashpot Model, *Cent. Eur. J. Energ. Mater*, **2012**, *9*(3), 189-199.

[5] Yaman H., Çelik V., Değirmenci E., Experimental Investigation of the Factors Affecting the Burning Rate of Solid Rocket Propellants, *Fuel*, **2014**, *115*, 794-803.

[6] Agrawal J.P., *High Energy Materials*, Wiley-VCH, Weinheim, **2010**, 320-324.

[7] Zalewski R., Pyrz M., Wolszakiewicz T., Modeling of Solid Propellants Viscoplastic Behavior Using Evolutionary Algorithms, *Cent. Eur. J. Energ. Mater.*, **2010**, *7*(4), 289-300.

[8] Zalewski R., Wolszakiewicz T., Bajkowski J., Temperature Influence on Fundamental Mechanical Properties of Homogeneous Solid Propellants, *Przemysl Chemiczny*, **2012**, *91*(9), 1830-1833.

[9] Wu X.G, Yan Q.L, Guo X, Qi X.F, Li X.J, Wang K.Q., Combustion Efficiency and Pyrochemical Properties of Micron-sized Metal Particles as the Components of Modified Double-base Propellant, *Acta Astronaut.*, **2011**, *68*, 1098-112.

[10] Frank G.J., Brockman R.A., A Viscoelastic-viscoplastic Constitutive Model for Glassy Polymers, *Int. J. Solids Struct.*, **2001**, *38*, 5149-64.

[11] Ho K., Krempl E., Extension of the Viscoplasticity Theory Based on Overstress (VBO) to Capture Non-standard Rate Dependence in Solids, *Int. J. Plasticity*, **2002**, *18*, 851-72.

[12] Zaïri F., Naït-Abdelaziz M., Woznica K., Gloaguen J.M., Constitutive Equations for

the Viscoplastic-damage Behaviour of a Rubber-modified Polymer, *Eur. J. Mech. A/Solids*, **2005**, *24*, 169-182.

[13] Zaïri F., Woznica K., Naït-Abdelaziz M., Gloaguen J.M., Elasto-viscoplastic Constitutive Equations for the Description of Glassy Polymers Behaviour at Constant Strain Rate, *J. Eng. Mater. Technol*., **2007**, *129*, 1-7.

[14] Colak O.U., Modeling Deformation Behavior of Polymers with Viscoplasticity Theory Based on Overstress, *Int. J. Plasticity*, **2005**, *21*, 145-60.

[15] Bodner S.R., Partom Y., Constitutive Equations for Elastic-viscoplastic Strain-hardening Materials, *J. Appl. Mech*., **1975**, *42*, 385-89.

[16] Rowley M.A., Thornton E.A., Constitutive Modeling of the Visco-plastic Reponse of Hastelloy-x and Aluminium Alloy 8009, *J. Eng. Mater. Technol*., **1996**, *118*, 19-27.

[17] Michalewicz Z., *Genetic Algorithms + Data Structures =Evolution Programs*, Springer, Berlin, **1992**.

[18] Lin J., Yang J., GA-based Multiple Objective Optimization for Determining Viscoplastic Constitutive Equations for Superplastic Alloys, *Int. J. Plasticity*, **1999**, *15*, 1181-96.

[19] Pyrz M., Zalewski R., Modeling of Granular Media Submitted to Internal Underpressure, *Mech. Res. Commun.*, **2010**, *37*(2), 141-144.

[20] Zalewski R., Pyrz M., Experimental Study and Modeling of Polymer Granular Structures Submitted to Internal Underpressure, *Mech. Mater.*, **2013**, *57*, 75-85.

[21] Hemin A., Messager T., Ayoub G., Zaïri F., Naït-Abdelaziz M., Zhengwei Q., Zairi F., A Two-phase Hyperelastic-viscoplastic Constitutive Model for Semi-crystalline Polymers: Application to Polyethylene Materials with a Variable Range of Crystal Fractions, *J. Mech. Behav. Biomed. Mater.*, **2014**, *37*, 323-332.

[22] Hemin A., Messager T., Zaïri F., Naït-Abdelaziz M., Large-strain Viscoelastic-viscoplastic Constitutive Modeling of Semi-crystalline Polymers and Model Identification by Deterministic/Evolutionary Approach, *Comput. Mater. Sci.*, **2014**, *90*, 241-252.

[23] Zalewski R., Constitutive Model for Special Granular Structures, *International Journal of Non-Linear Mechanics*, **2010**, *45*(3), 279-285.